APPLICATION NOTE

Characterize Immune Checkpoint Proteins and T Cell Exhaustion Using Multiplex IHC

Gaining molecular insights from the tumor microenvironment

Advantages of CST antibodies for IHC	
Disease Relevance	Targets relevant for translational cancer research in human and mouse.
Validation	CST antibodies are developed and validated in-house, ensuring specificity and performance in IHC.
Versatility	Work with FFPE tissue samples, automated IHC platforms, and both chromogenic and multiplexed fluorescent IHC protocols.
Value	Get more insights from precious tissue samples, including co-localization.

Introduction

Advances in immuno-oncology have successfully led to novel cancer therapeutics with favorable patient responses that are more durable than conventional cytotoxic chemotherapy (1). However, not all patients respond to immunotherapy; therefore investigators are trying to identify clinically relevant biomarkers with the goal of developing therapeutics based on personalized medicine (2,3).

Spatial localization of multiple biomarkers is critical when cataloging subsets of immune infiltrate and cancer cells and their interactions in the tumor microenvironment. Multiplexed assays are required for investigations of multiple therapeutic targets and predictive biomarkers in limited and valuable patient samples. For these reasons, fluorescent multiplex immunohistochemistry (mIHC), which enables detection of 6 or more proteins/biomarkers in formalin-fixed, paraffin-embedded (FFPE) tissue samples, is a valuable tool for immuno-oncology.

In mIHC as well as in single/dual-plex chromogenic IHC approaches, using application-validated antibodies against relevant targets is crucial in order to obtain reliable results. Antibodies validated for IHC from CST enable investigators to get more information about biomarker expression, localization, interaction, and disease context.

This application note explores the protocol and technical considerations for selecting and using antibodies in mIHC to assess immune checkpoint proteins and T cell exhaustion in FFPE tissue samples.

Background and Results

The tumor microenvironment is the site of interactions between evolving cancer cells and infiltrating immune cells, including CD8+ cytotoxic T cells, CD4+ helper T cells, and others. T cells normally become activated after encountering immunogenic antigens presented by major histocompatibility complex molecules on the surface of mutated cancer cells or antigen-presenting cells. Some cancers acquire the ability to evade immune detection by manipulating the expression of immune checkpoint proteins, including ligands of PD-1, CTLA-4, TIM-3, and many other proteins (4-6). Inhibitory immune checkpoint ligands normally mediate immune self-tolerance and regulate the amplitude of immune responses to pathogens in healthy tissue, but are often upregulated in cancer cells to "turn off" T cell activation. Therefore, therapeutic strategies focusing on immune checkpoint signaling have been the subject of intense research and drug development efforts (1). Molecular profiling of both immune checkpoint markers and immune cell phenotyping markers is key to understanding the complex tumor microenvironment and the development of tailored, combinatorial therapeutic interventions. Antibodies targeting six proteins involved in immune checkpoint regulation (**Table 1**) were analyzed in multiplexed IHC, and are shown as both merged and individual channels (**Figure 1**).

In successful immune responses, activated T cells and natural killer cells attack and clear all cells infected by pathogens or tumor cells, while macrophages clear the debris. Subsequently, most of the T cells die while a subset undergoes differentiation to memory T cells that self-renew in the absence of antigen. Chronic exposure to antigen leads to the phenomenon of T cell exhaustion. Exhausted T cells progressively lose their capacity to kill tumor cells, proliferate, and produce cytokines. They also exhibit elevated expression of immune checkpoint proteins including PD-1, LAG3, and TIM-3 that are partly responsible for the exhausted phenotype. The immune checkpoint protein VISTA is expressed on exhausted T cells and, to a greater degree, on co-infiltrating CD68+ macrophages (7,8). The functional severity of T cell exhaustion correlates with the number and magnitude of immune checkpoint protein expression changes (9–11). T cell exhaustion is of particular interest because interventions to reverse it have been shown to revive extant immune functions in the tumor microenvironment (12,13). Antibodies targeting TIM-3, PD-1, and LAG3 to mark T cell exhaustion, and antibodies targeting CD8, CD68, and cytokeratin for spatial context (**Table 2**) were analyzed in multiplexed IHC (**Figure 2**).

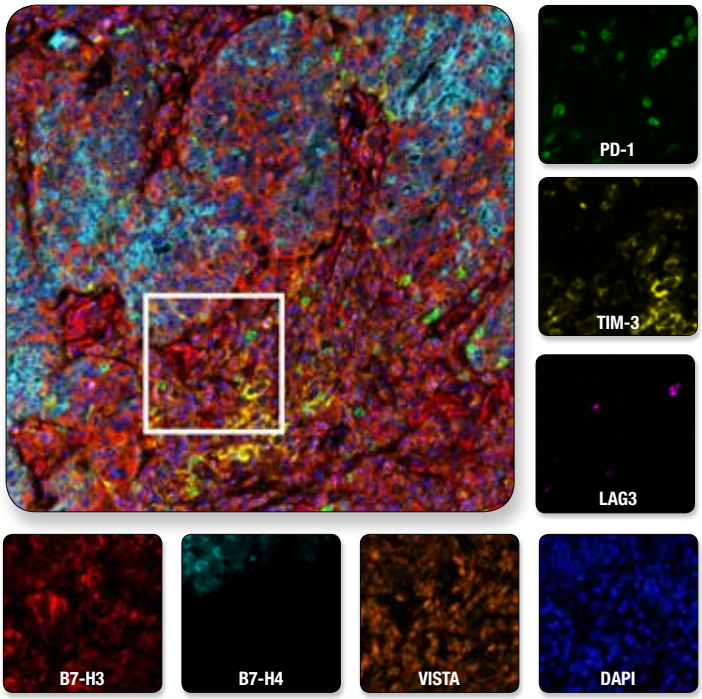

Figure 1: Multiplexed IHC analysis of ovarian serous carcinoma tissue probed with a 6-plex panel for co-inhibitory immune checkpoint proteins, plus DAPI to label nuclei. Multiplexed image of all seven channels (upper left) is shown with a region of interest (white box in upper left) from which the individual channels are displayed.

Multiplex IHC: Tumor Microenvironment

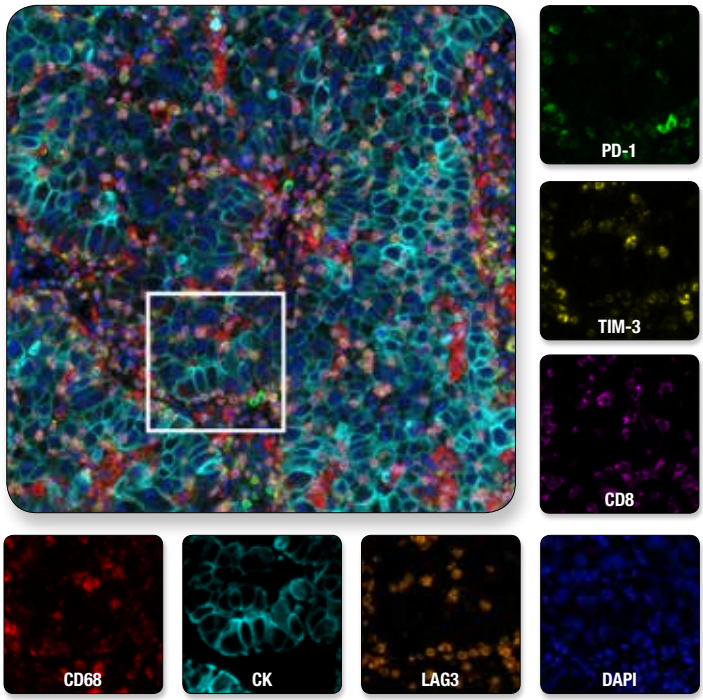

Figure 2: Multiplexed IHC analysis of non-small cell lung carcinoma probed with a 6-plex panel for T cell exhaustion proteins, plus DAPI to label nuclei. Multiplexed image of all seven channels (upper left) is shown with a region of interest (white box in upper left) from which the individual channels are displayed.

Methods

For questions about how to customize your protocol using our full catalog of over 700 antibodies approved for IHC, please contact technical support: www.cellsignal.com/support

Multiplexed IHC employs a serial labeling strategy. Following incubation of tissue with primary antibody, HRP-conjugated secondary antibodies catalyze deposition of tyramide-fluorophore complexes. The fluorophores remain covalently bound to the tissue while the antibodies are removed via microwave treatment between labels. Note that the removal of primary antibodies after each labeling round allows for the use of multiple antibodies from the same host species (e.g., rabbit).

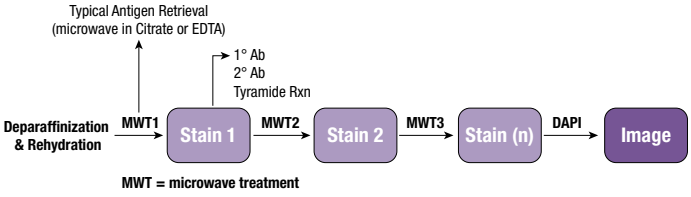

Figure 3: Schematic representation of the fluorescent mIHC workflow

FFPE tissue sections were processed and analyzed for mIHC in accordance with the protocol (illustrated above).

1. **Deparaffinization/Rehydration:** To prepare for antigen retrieval, tissue sections were deparaffinized with xylene, followed by rehydration with 100% ethanol, 95% ethanol, and dH20.
2. **Antigen Retrieval:** Extensive optimization was performed to ensure maximal unmasking of each epitope to allow for efficient binding of the primary antibody. See Optimization section for details.
3. **Antibody Titration:** The optimal dilution for each primary antibody was determined empirically to ensure maximal fluorescence intensity and minimal background signal for each target of interest. See Optimization section for details.
4. **Staining:** Incubation with primary antibodies was performed under humidified conditions at room temperature using SignalStain® Antibody Diluent #8112. Subsequent incubation with either SignalStain® Boost IHC Detection Reagent (HRP, Mouse) #8125 or SignalStain® Boost IHC Detection Reagent (HRP, Rabbit) #8114, as appropriate, was performed.
5. **Image Acquisition/Analysis**: The Mantra® Quantitative Pathology Workstation system was used for multispectral imaging. Image analysis was performed using the InForm® Image Analysis software package.

Table 1: Co-Inhibitory Immune Checkpoint Antibody Selections

ORDER	TARGET	CST ANTIBODY	DILUTION	FLUOROPHORE
1st	PD-1	PD-1 (D4W2J) XP® Rabbit mAb #86163	1:600	FITC
2nd	B7-H3	B7-H3 (D9M2L) XP® Rabbit mAb #14058	1:250	Cy™5
3rd	LAG3	LAG3 (D2G40™) XP® Rabbit mAb #15372	1:600	Alexa Fluor® 594
4th	TIM-3	TIM-3 (D5D5R™) XP® Rabbit mAb #45208	1:400	Alexa Fluor® 555
5th	VISTA	VISTA (D1L2G™) XP® Rabbit mAb #64953	1:50	Cy™5.5
6th	B7-H4	B7-H4 (D1M8I) XP® Rabbit mAb #14572	1:25	Alexa Fluor® 350

Table 2: T Cell Exhaustion Antibody Selections

ORDER	TARGET	CST ANTIBODY	DILUTION	FLUOROPHORE
1st	TIM-3	TIM-3 (D5D5R™) XP® Rabbit mAb #45208	1:400	Alexa Fluor® 555
2nd	CD8	CD8α (C8/144B) Mouse mAb (IHC Specific) #70306	1:8,500	Alexa Fluor® 594
3rd	PD-1	PD-1 (EH33) Mouse mAb (IHC-Specific) #43248	1:500	FITC
4th	CD68	CD68 (D4B9C) XP® Rabbit mAb #76437	1:10,000	Cy™5
5th	LAG3	LAG3 (D2G40™) XP® Rabbit mAb #15372	1:200	Cy™5.5
6th	CK (cytokeratin)	Pan-Keratin (C11) Mouse mAb #4545	1:250	Alexa Fluor® 350

Multiplex IHC: Tumor Microenvironment

Optimization

Titration: Prior to performing a multiplex experiment, the optimal concentration of each primary antibody needs to be determined in a singleplex setting. To this end, an extensive dilution series of TIM-3 (D5D5R™) XP® Rabbit mAb was used to determine the dilution point that yields to maximal fluorescence signal intensity combined with the highest signal to noise (S/N) ratio (**Figure 4**). This was done using sections of paraffin-embedded cell pellets known to express TIM-3 at high levels (Daudi) as well those with negligible levels of TIM-3 expression (Jurkat) as positive and negative controls, respectively. Optimal S/N is obtained at a 1:400 dilution. We highly recommend applying this approach to establish the optimal dilutions for all antibodies to be used in a multiplex experiment.

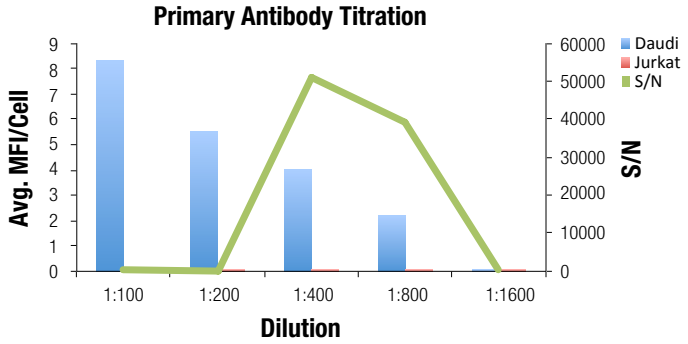

Figure 4: Mean fluorescence intensity (MFI) and signal/noise ratio (S/N) as a function of TIM-3 (D5D5R ™) XP® Rabbit mAb #45208 dilution. SignalStain® Boost IHC Detection Reagent (HRP, Rabbit) #8114 and tyramide-FITC conjugate were used for detection.

Order Optimization: The order in which antibodies in a multiplex panel are applied to a tissue section must be optimized to ensure that multiple rounds of heating do not compromise the integrity of the epitope of interest. For the purposes of order optimization, note that each tissue section was labeled/stained only once and subjected to microwave treatment the same number of times irrespective of labeling order. TIM-3 (D5D5R™) XP® Rabbit mAb exhibits progressive reduction of signal dependent on labeling order, likely due to epitope loss; however, the degree of reduction is not so great as to prevent its use in intermediate positions (**Figure 5**). Our protocols include TIM-3 labeling in the 1st step in the T cell exhaustion panel and in the 4th position in the co-inhibitory panel (**Tables 1-2**). The optimal positioning of an antibody is ultimately determined by the results of this matrix, in addition to those of the other antibodies in the panel, such that all signal intensities are balanced in the final panel.

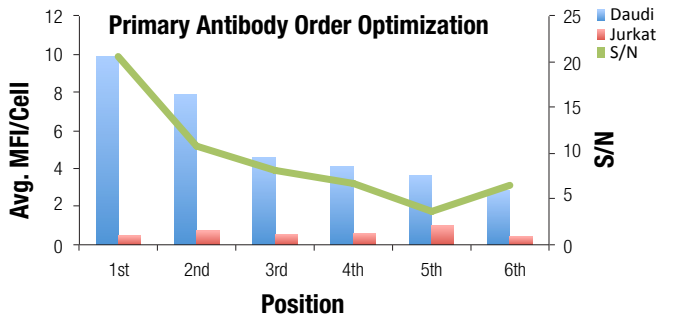

Figure 5: Mean fluorescence intensity (MFI) and signal/noise ratio (S/N) as a function of TIM-3 (D5D5R™) XP® Rabbit mAb #45208 labeling order.

Fluorophore Pairing: The objective of this optimization step is to achieve a balance of signal intensities within the panel so that the fluorescence signal originating from targets of high abundance does not crowd out the signal originating from targets with lower abundance. To this end, it is good practice to pair antibodies detecting targets with low expression with the brightest fluorophores and vice versa (**Figure 6**). We recommend analyzing a matrix composed of optimized primary antibodies paired with each available fluorophore in order to ascertain this optimal balance both with respect to signal intensity and S/N ratio.

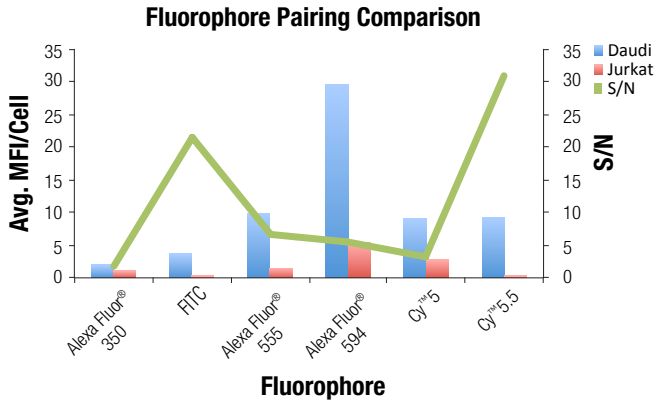

Figure 6: Mean fluorescence intensity (MFI) and signal/noise ratio (S/N) of TIM-3 (D5D5R™) XP® Rabbit mAb #45208 as a function of fluorophore pairing.

Conclusion

In-depth characterization of the tumor microenvironment can be acheived using mIHC. The data shown here demonstrate, the capability to image six biomarkers plus DAPI in FFPE tissue samples. Rational optimization of experimental parameters including antibody dilutions, order of staining, and fluorophore pairing is recommended when designing mIHC panels. Further analysis of biomarker expression patterns, for example co-expression or mutual exclusivity in the same cell or in adjacent cells, is also possible with mIHC.

References

1. Sharma, P. and Allison, J.P. (2015) *Cell* 161, 205–14.
2. Mahoney, K.M. and Atkins, M.B. (2014) *Oncology* (Williston Park) 28 (suppl 3), 39–48.
3. Masucci, G.V. et al. (2016) *J Immunother Cancer* 4, 76.
4. Pardoll, D.M. (2012) *Nat Rev Cancer* 12, 252–64.
5. Schildberg, F.A. et al. (2016) *Immunity* 44, 955–72.
6. Anderson, A.C. et al. (2016) *Immunity* 44, 989–1004.
7. Lines, J.L. et al. (2014) *Cancer Res* 74, 1924–32.
8. Liu, J. et al. (2015) *Proc Natl Acad U S A* 112, 6682–7.
9. Blackburn, S.D. et al. (2009) *Nat Immunol* 10, 29–37.
10. Jin, H.T. et al. (2010) *Proc Natl Acad U S A* 107, 147233–8.
11. Wherry, E.J. and Kurachi, M. (2015) *Nat Rev Immunol* 15, 486–99.
12. Barber, D.L. et al. (2006) *Nature* 439, 682–7.
13. Nguyen, L.T. and Ohashi, P.S. (2015) *Nat Rev Immunol* 15, 45–56.